



OPEN

Historic evolution of population exposure to heatwaves in Xinjiang Uygur Autonomous Region, China

Diwen Dong^{1,3,4,5}, Hui Tao¹ & Zengxin Zhang^{1,2}✉

Heatwaves have pronounced impacts on human health and the environment on a global scale. Although the characteristics of heatwaves has been well documented, there still remains a lack of dynamic studies of population exposure to heatwaves (PEH), particularly in the arid regions. In this study, we analyzed the spatio-temporal evolution characteristics of heatwaves and PEH in Xinjiang using the daily maximum temperature (T_{max}), relative humidity (RH), and high-resolution gridded population datasets. The results revealed that the heatwaves in Xinjiang occur more continually and intensely from 1961 to 2020. Furthermore, there is substantial spatial heterogeneity of heatwaves with eastern part of the Tarim Basin, Turpan, and Hami been the most prone areas. The PEH in Xinjiang showed an increasing trend with high areas mainly in Kashgar, Aksu, Turpan, and Hotan. The increase in PEH is mainly contributed from population growth, climate change and their interaction. From 2001 to 2020, the climate effect contribution decreased by 8.5%, the contribution rate of population and interaction effects increased by 3.3% and 5.2%, respectively. This work provides a scientific basis for the development of policies to improve the resilience against hazards in arid regions.

Heatwaves are generally defined as extended periods of extremely high temperatures. It can have catastrophic impacts on human health, infrastructure, agricultural ecosystems, and the national economy^{1–3}. For example, the intense heatwaves resulted in more than 70,000 deaths in Europe in 2003⁴, the railway infrastructure in Australia was damaged in 2009⁵, and the crop failure in Russia in 2010 was about 25%⁶. Especially, in recent years, China has been hit by heatwaves several times. Shanghai and Xinjiang suffered unprecedented heatwaves in 2013 and 2015, respectively^{7,8}. According to the 2020 China report of The Lancet Countdown on health and climate change, heatwave-related mortality has a four-fold increase from 1990 to 2019 in China⁹. Under the background of global climate change, the adverse impacts of increasing heatwaves on human health and socio-economics will become more serious^{10,11}. However, few studies explored the spatial heterogeneity of heatwaves and the dynamic variation of population exposure simultaneously. Thus, there is an urgent requirement to elucidate the spatio-temporal evolution of heatwaves and quantify the deleterious impacts of heatwave exposure for providing scientific insights for coping with climate change.

Currently, heatwaves have attracted widespread attention from government departments and the scientific community. Most heatwave investigations includes limited metrics such as frequency, intensity, and duration^{12,13}. Prolonged exposure to heatwaves can endanger human health¹⁴, thus more detailed studies of the adverse effects of heatwaves on population is required¹⁵. Previous studies have typically linked heatwaves to human health through heat-related morbidity and mortality data^{16,17}. Hajat et al.¹⁸ investigated that death rate increased by 3.34% for every degree of temperature increase. Nevertheless, the heat-related mortality is related to climate and population. Jones et al.¹⁹ calculated population exposure to heatwaves spatially, in other to quantify the influence of natural hazards. It is difficult to deeply analyze the dynamics of spatial population exposure on the basis of previous population data by administrative regions. This limitation can be effectively overcome by high-resolution gridded population datasets²⁰.

Heatwaves in the Xinjiang Uygur Autonomous Region have increased significantly over the last few decades^{21,22}, being expected to occur more continually and intensely in the future²³. Previous studies in Xinjiang identifies heatwaves by daily maximum. In addition to the high temperature, human comfort and health are also

¹State Key Laboratory of Desert and Oasis Ecology, Xinjiang Institute of Ecology and Geography, Chinese Academy of Sciences, Urumqi 830011, China. ²Joint Innovation Center for Modern Forestry Studies, College of Forestry, Nanjing Forestry University, Nanjing 210037, Jiangsu, China. ³College of Ecology and Environment, Xinjiang University, Urumqi 830046, China. ⁴University of Chinese Academy of Sciences, Beijing 100049, China. ⁵College of Statistics & Data Science, Xinjiang University of Finance & Economics, Urumqi 830012, China. ✉email: nfzhang@163.com

affected by the relative humidity (RH), wind speed and the solar radiation^{24,25}. Furthermore, as the RH increases, some heat-related deaths happen at relatively low temperatures, illustrating that the RH play another significant role in identifying heatwaves^{26,27}. Currently, the climate in Xinjiang has exhibited a trend of ‘warming-wetting’^{28,29}. There might be great uncertainty when attempting to estimate heatwaves without considering the RH. Hence, the indices combining temperature and RH are more suitable for characterizing heatwaves in Xinjiang.

Compared with the characteristics of heatwaves, few studies have focused on the population exposure to heatwaves (PEH) in Xinjiang. Even though some relevant studies in large scale regions have included Xinjiang, the assessment results do not accurately reflect the evolution of PEH in Xinjiang³⁰. Xinjiang is at the heart of the Belt and Road Initiative, with higher population growth than the national average. Therefore, studies on the PEH in Xinjiang are necessary. The spatial distribution of population in Xinjiang is influenced by the oasis and typical of the population distribution in arid areas³¹. Studying the characteristic of heatwave and PEH in Xinjiang can provide a scientific basic for active response to climate change in arid regions.

In this paper, we investigate the dynamic changes of heatwaves and PEH using a long time series of high-resolution population data and further quantify the factors driving the PEH. The primary goal of this study includes: (1) revealing the spatial and temporal evolution of heatwaves under the ‘warming-wetting’ trends in Xinjiang, (2) assessing the dynamic changes of population exposure under the rapidly increasing heatwaves and population in Xinjiang, and (3) quantifying the impacts of climate and population changes on the PEH in Xinjiang. This work provides the useful scientific support for the design of strategies to deal with climate change in Xinjiang.

Results

Interannual variability of heatwave. The temporal variability of annual heatwave in Xinjiang for the period 1961–2020 is presented in Fig. 1. The heatwave frequency (HWF) (Fig. 1a) and heatwave season length (HWS) (Fig. 1c) shows fluctuating changes with an abrupt change around 1994. The mean values for HWF and HWS increases by 1.04 times and 10.9 days after mutation, respectively. For the heatwave duration (HWD) (Fig. 1b), no significant change is noticed for the whole series and 2015 is the year with the longest HWD (5.8 days). Besides the increase HWF and HWD, the increase in heatwaves is also associated with the changes in first heatwave timing (HWFT) (Fig. 1d) and last heatwave timing (HWLT) (Fig. 1e). The HWFT begins mainly in June and the difference between the earliest and the latest onset year is 41 days. While the HWLT ends in August for most years. The latest year for the end of HWLT between 1961 and 2020 is 1997. In general, not only the HWF and HWS are increasing in Xinjiang, but the HWFT is advancing and HWLT is postponing.

Heatwave spatial distribution and variations. Heatwaves have occurred in most areas of Xinjiang from 1961 to 2020. The distribution of heatwaves exhibits significant spatial heterogeneity. The high values of HWF (Fig. 2a), HWD (Fig. 2b), and HWS (Fig. 2c) are concentrated in Turpan, Hami, and the eastern portion of Bayingolin. Simultaneously, the HWFT begins earliest and the HWLT ends latest in these areas (Fig. 2d,e). The low values are broadly distributed in Altay, the margin of the Junggar Basin, and the margin of the Tarim Basin.

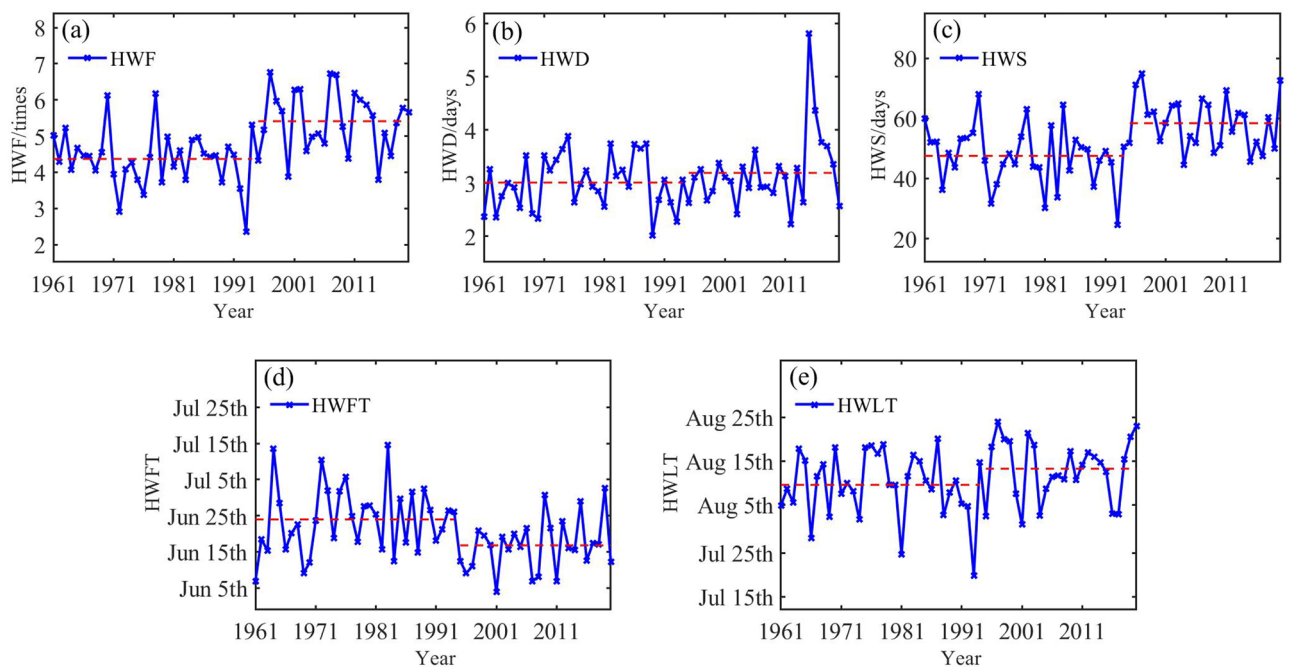


Figure 1. Times series of (a) heatwave frequency (HWF), (b) heatwave duration (HWD), (c) heatwave season length (HWS), (d) first heatwave timing (HWFT), and (e) last heatwave timing (HWLT) in Xinjiang from 1961 to 2020. Dashed lines indicate their average of the corresponding time period.

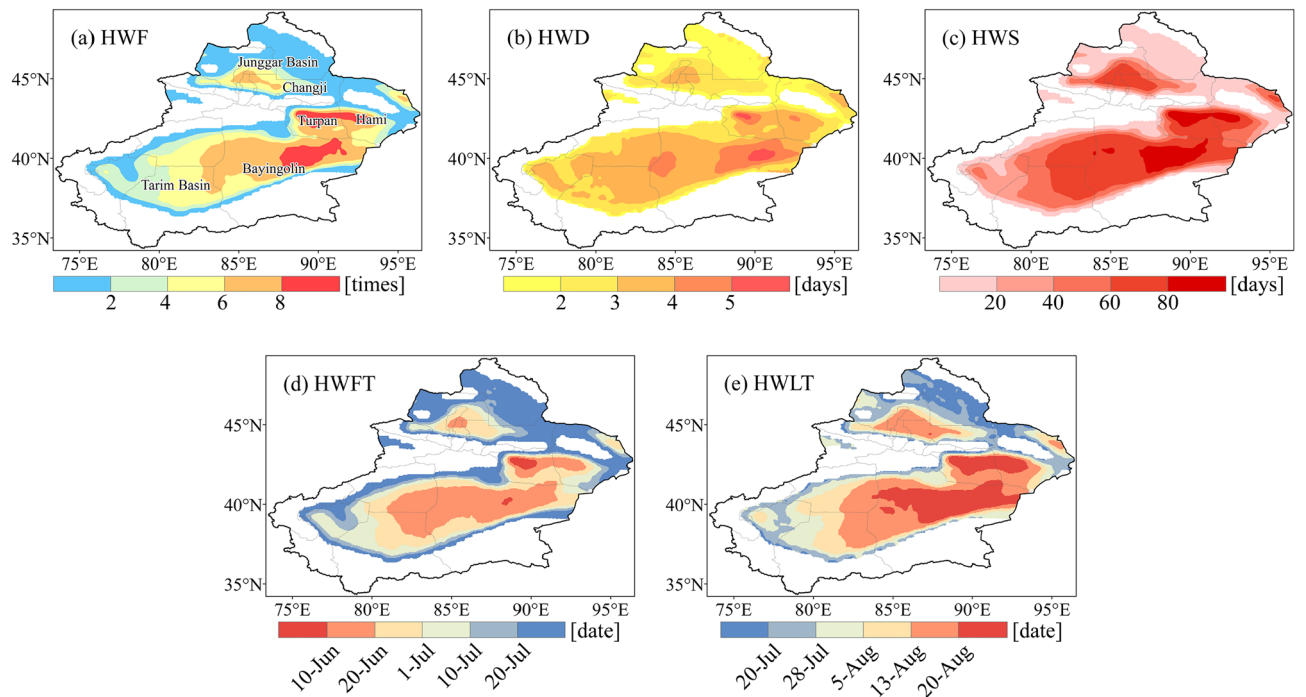


Figure 2. Spatial distribution of annual averaged (a) heatwave frequency (HWF), (b) heatwave duration (HWD), (c) heatwave season length (HWS), (d) first heatwave timing (HWFT), and (e) last heatwave timing (HWLT) in Xinjiang from 1961 to 2020.

High-altitude mountains such as the Kunlun, Tianshan, and Altai Mountains have never been hit by heatwaves from 1961 to 2020. Our study revealed that most heatwaves in Xinjiang are occurred in areas below the altitude of 1500 m, and never occurred in areas above the altitude above 2500 m.

Figure 3 shows the spatial pattern trends in heatwaves. Significantly increasing trends ($p < 0.05$) in both the HWF (Fig. 3a) and HWS (Fig. 3c) can be observed in many areas of Xinjiang, such as the Tarim Basin, Changji,

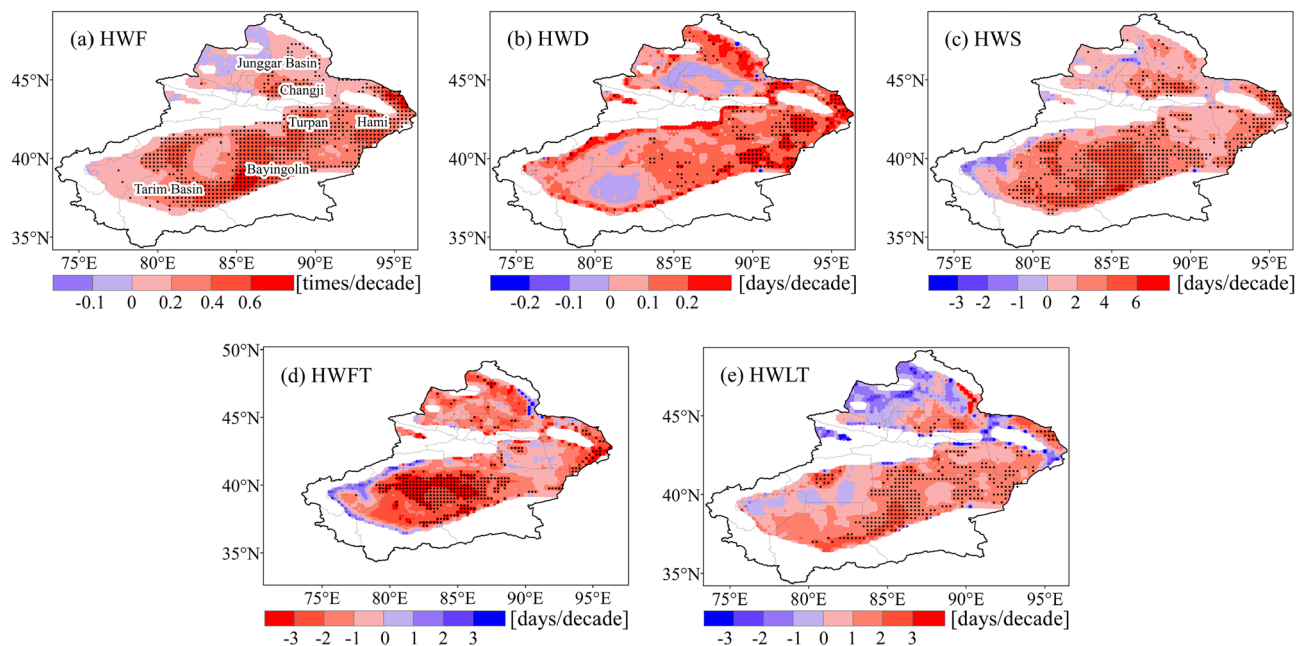


Figure 3. Trends of (a) heatwave frequency (HWF), (b) heatwave duration (HWD), (c) heatwave season length (HWS), (d) first heatwave timing (HWFT), and (e) last heatwave timing (HWLT) in Xinjiang from 1961 to 2020. Stippling denotes statistically significant trends ($p < 0.05$).

Hami and the Southern Junggar Basin. However, the remarkable increase of the HWD (Fig. 3b) are concentrated in Hami and the eastern portion of Bayingolin. Similarly, the advanced HWFT (Fig. 3d) and the delayed HWLT (Fig. 3e) are most notable in the Tarim Basin. Overall, heatwaves are more frequent, longer lasting, and more intense in most areas of Xinjiang.

Heatwave grades. From 1961 to 2020, heatwaves in Xinjiang typically occurred between May and August (Fig. 4). In terms of occurrence times, the light heatwaves (LHW) (Fig. 4a) occurs earliest (beginning on May 21 on average), which is 13 and 29 days earlier than the appearance of moderate heatwaves (MHW) (Fig. 4b) and strong heatwaves (SHW) (Fig. 4c), respectively. Meanwhile, the LHW is the latest ending (August 31 on average). From the perspective of the area and duration, Xinjiang is primarily affected by LHW, followed by MHW, and the least by SHW. However, 2015 is a very unique year. The number of SHW days not only the highest from 1961 to 2020 (8.2 days), but more than the number of MHW days in 2015.

Different grades of heatwave days are increasing significantly in most parts of Xinjiang, regardless of the grade (Fig. 5). The areas of significant increase in LHW are widely distributed in Aksu, Bayingolin, Changji, Turpan, and Hami. While the areas where MHW and SHW increase significantly are concentrated in Bayingolin, Turpan, and Hami. The area of heatwaves affected by different grades is LHW > MHW > SHW. In other words, areas where LHW occurs do not necessarily have MHW and SHW, while areas where SHW occurs must have had LHW. However, this indicates that not all areas where heatwaves occurred are hit by SHW, which is particularly obvious in Yili and Altay.

Analysis of PEH and its influencing factors. Exposure is an important indicator for disaster risk assessment, which is of great significance for conducting high-temperature warning work³². It can be observed from

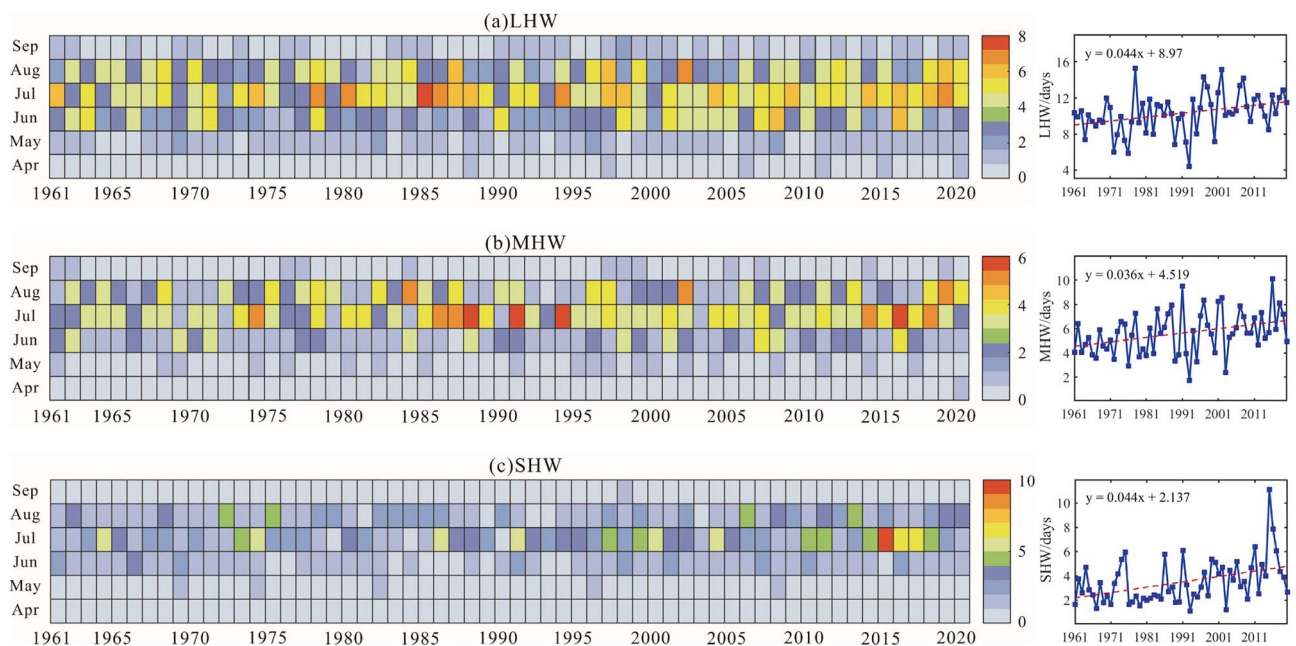


Figure 4. Times series of (a) light heatwaves (LHW), (b) moderate heatwaves (MHW), and (c) strong heatwaves (SHW) in Xinjiang from 1961 to 2020. Dashed lines indicate corresponding linear trends.

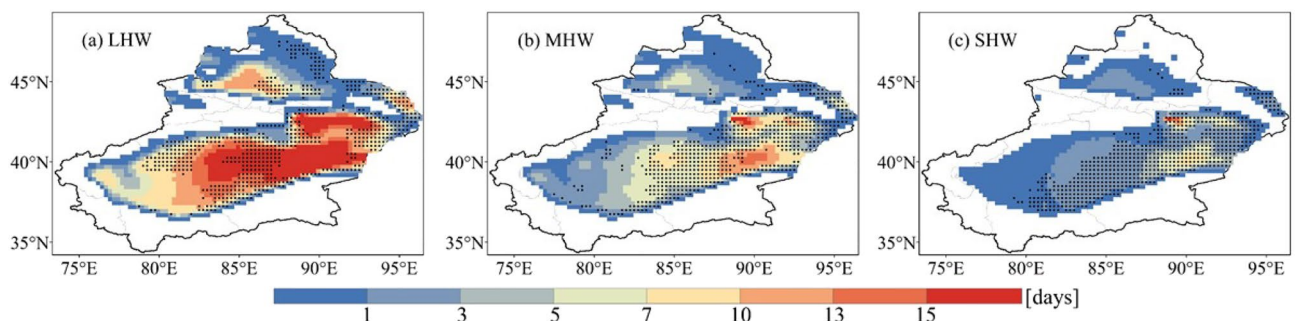


Figure 5. Spatial distribution of (a) light heatwaves (LHW), (b) moderate heatwaves (MHW), and (c) strong heatwaves (SHW) in Xinjiang from 1961 to 2020. Stippling denotes statistically significant trends ($p < 0.05$).

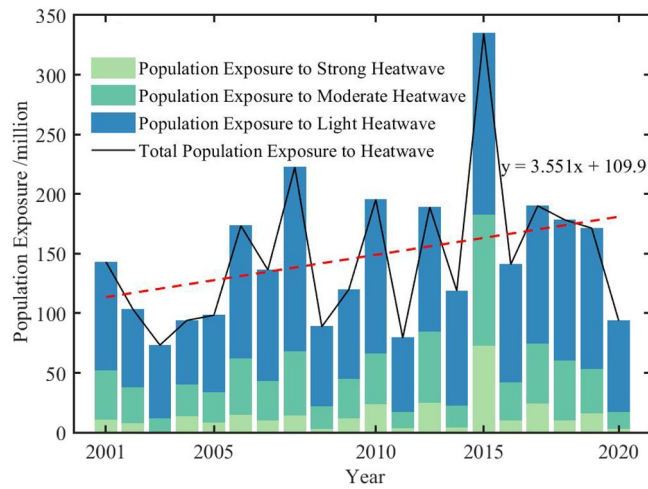


Figure 6. Population exposure to different grades of heatwaves in Xinjiang from 2001 to 2020. Dashed line indicates corresponding linear trends.

Fig. 6 that the PEH in Xinjiang is primarily affected by the LHW, and less affected by the MHW and SHW. The total PEH exhibits an increasing trend from 2001 to 2020. The year with the highest PEH in Xinjiang is not 2020 with the largest population, but rather 2015 with the longest HWD. This indicates that in addition to population growth, climate change also have an impact on changes in the PEH.

The spatial distribution of PEH shows significant geographical heterogeneity, which is consistent with the spatial distribution of the population (Fig. 7). The spatial pattern of PEH in Xinjiang is similar for different periods.

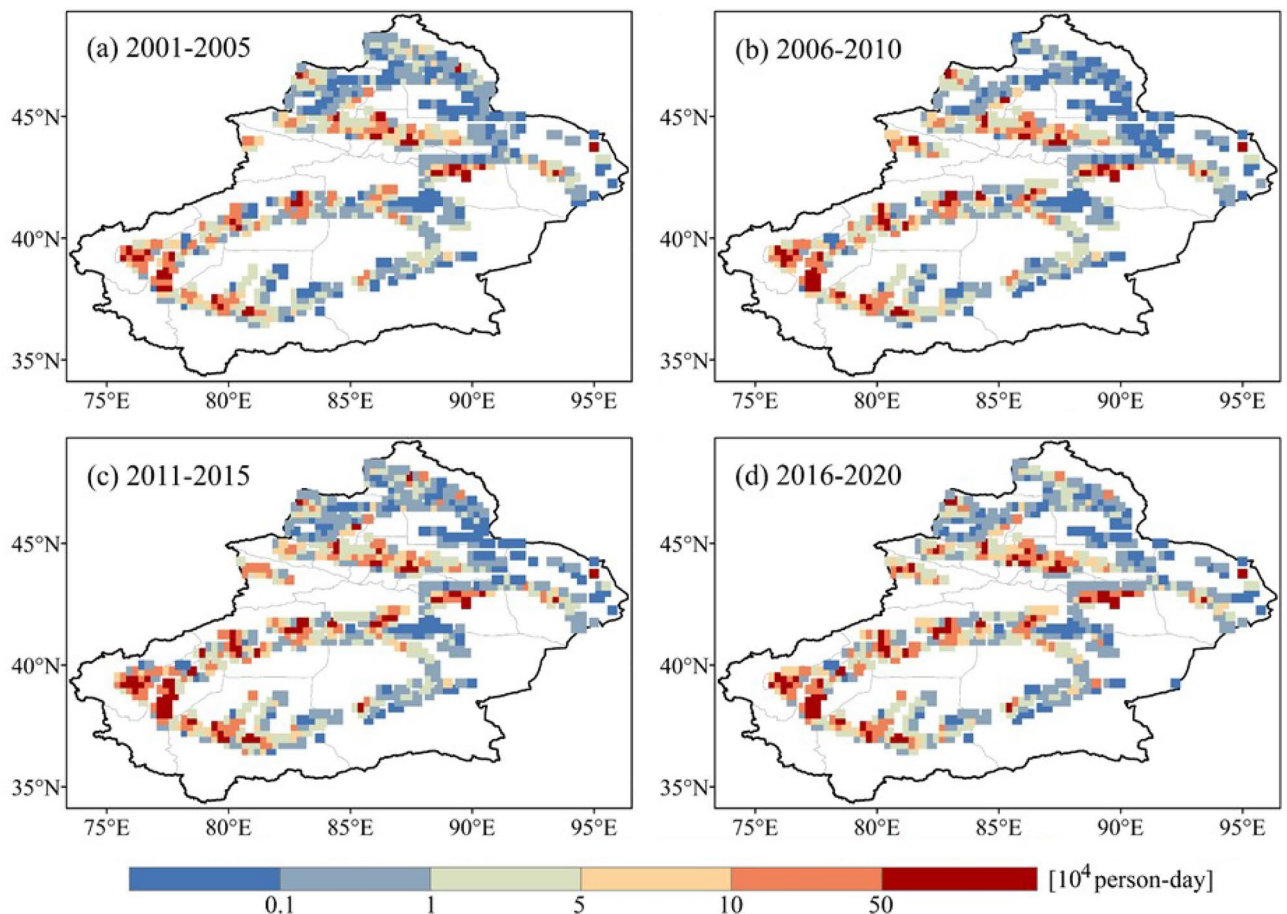


Figure 7. Spatial distribution of population exposure to heatwaves (PEH) in Xinjiang.

Areas with high PEH (10^5 person-days or more) are mainly located in Kashgar, Aksu, Turpan, and Hotan. The areas of extremely low PEH (10^3 person-days and below) are broadly distributed in Altay, the margin of the Junggar Basin, and the eastern portion of the Tarim Basin. Although the hinterlands of the Tarim and Junggar Basins are subject to frequent heatwaves, there is no PEH due to the absence of a population.

To further investigate the variation of PEH in Xinjiang, we compared the PEH in other periods with the T0 period (Fig. 8). We found that in densely populated areas (e.g., Hotan, Kashgar, and Aksu), the increase in PEH is considerable. The PEH in Bayingolin do not increase noticeably, while it does decrease in Altay.

The increase in PEH is mainly contributed from population growth, climate change and their interaction. To explore the relative importance, we evaluated the rate of contribution to PEH changes for each factor. Table 1 indicates that the contribution rate of the climate effect tends to decrease over time (8.5%). Simultaneously, the contribution rate of the population and interaction effects gradually increased by 3.3% and 5.2%, respectively. In conclusion, the climate effect is dominant over population and interaction effects in Xinjiang.

Heatwave in typical year. Xinjiang suffered the severest heatwave and the highest PEH in 2015 (Fig. 9). Figure 10 shows clearly that high temperatures occurred widely in Xinjiang in 2015 and also concentrated in mid to late July. Consecutive days of Tmax exceeded the historical day, which is consistent with the results of this study.

Xinjiang is located at the mid-latitudes in the Northern Hemisphere, where temperatures will continue to rise under the steady control of high-pressure systems⁸. Figure 11 illustrates the evolution of the geopotential height

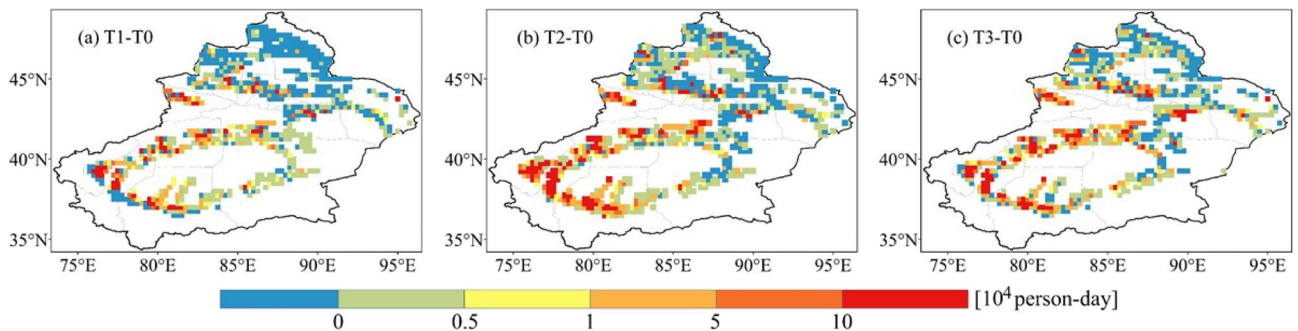


Figure 8. Changes in population exposure to heatwaves (PEH) for different periods (a 2006–2010, b 2011–2015, and c 2015–2020) compared with the base period (2001–2005).

Period	Population exposure change (10^6) person-days	Contribution rate of influencing factors (%)		
		Climate effect	Population effect	Interaction effect
T1–T0	38	53.9	37.8	8.3
T2–T0	94	48.5	39.1	12.4
T3–T0	65	45.4	41.1	13.5

Table 1. Contribution rates to population exposure changes for each factor.

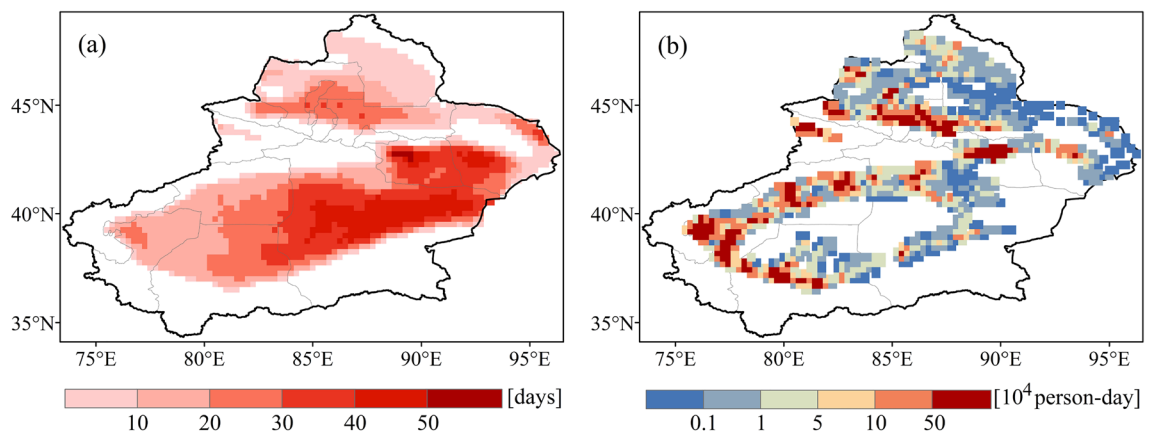


Figure 9. (a) Heatwave days in Xinjiang for 2015. (b) Population exposure to heatwaves in Xinjiang for 2015.

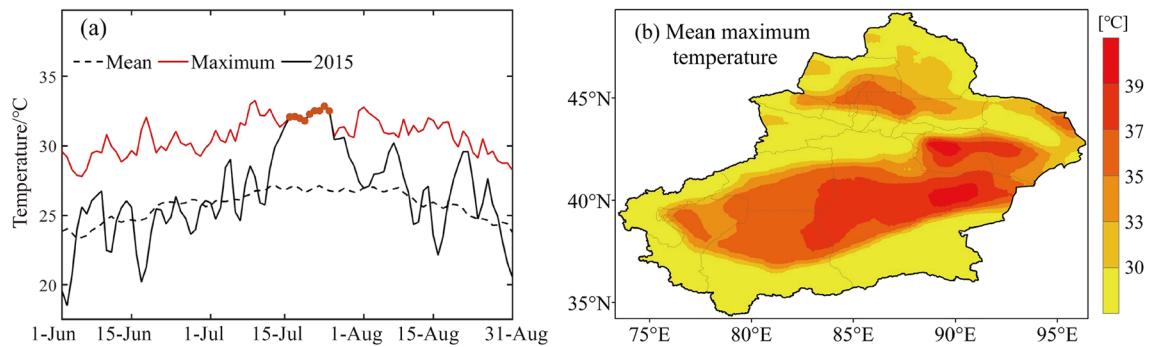


Figure 10. (a) Variation of daily maximum temperature (T_{\max}) in Xinjiang. The red solid line represents the maximum values of T_{\max} from 1961 to 2020. The black solid line represents the maximum values of T_{\max} in 2015. Red dots represent the maximum values of T_{\max} in 2015 that is the maximum from 1961 to 2020. Black dashed line represents T_{\max} averaged from 1961 to 2020. (b) Spatial distribution of the T_{\max} in Xinjiang for July 2015.

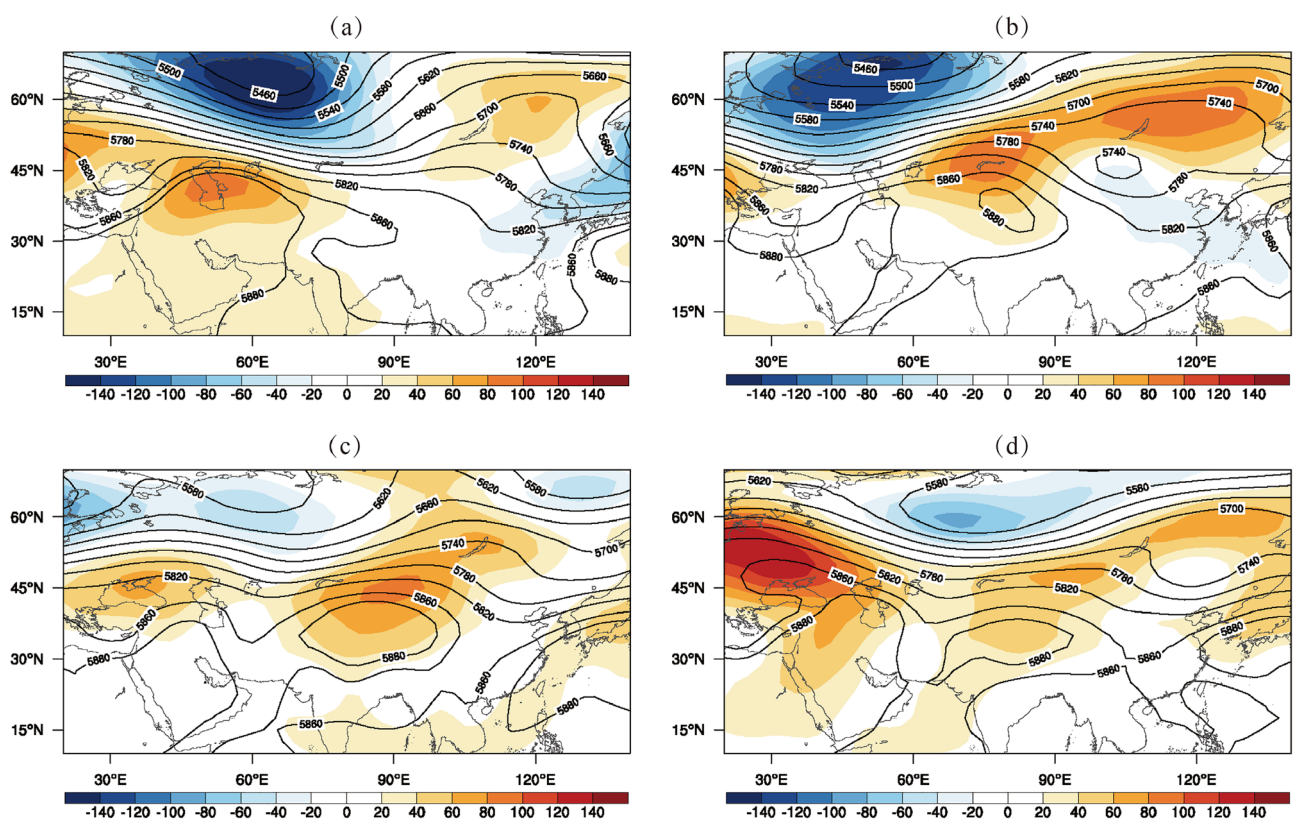


Figure 11. The geopotential height fields in (a) early July, (b) mid-July, (c) late July, and (e) early August for 2015.

field at 500 hPa from July to early August, 2015. We find the center of high pressure over the Iranian plateau shifts eastwards to Xinjiang, then remains stable and gets strengthened over Xinjiang, followed by the southward shift and getting weakened. The evolution of this Iranian high pressure coincides with corresponding changes in the high temperatures in Xinjiang. Therefore, the eastward shift of Iranian high pressure and its control of Xinjiang is the direct cause of this heatwave.

Discussion

This study examines the dynamic changes of heatwaves and PEH using a long time series of high-resolution population data and further quantifies the factors causing the PEH changes. By analyzing heatwave metrics, the spatio-temporal evolution pattern of heatwaves in Xinjiang has been comprehensively captured. The abrupt change point of heatwaves in 1994 is observed, coinciding with that in annual T_{\max} of Xinjiang occurring in the 1990s³³. Chen et al.³⁴ discovered an increase in the number of high-temperature days in Xinjiang when the South Asian high (SAH) is strong and its central area is located northwards. The increase in high temperatures

could trigger the corresponding increase in relative humidity. This could have an impact on heatwaves in these areas. China suffered severe heatwaves due to a super El Niño event that occurred in 1997³⁵, as well as the maximum values of HWF and HWS in Xinjiang occurred in the same year. This suggests that changes in heatwaves in Xinjiang is linked to El Niño event.

Because of the uneven global warming, the distribution of heatwaves have significant spatial heterogeneity. In this study, we found that the Eastern Tarim Basin, Turpan, and Hami are the most heatwave-prone, with the most significant increases in heatwaves. This is not only related to the high temperatures due to the low altitudes, also correlated with atmospheric circulation³⁶. For example, Mao et al.⁸ discovered the eastward shift of Iranian high pressure led to the longest lasting and most widespread heatwave of Xinjiang in 2015. In addition, the distribution of heatwaves is influenced by land use and latitude^{37,38}. Heatwaves in northern Xinjiang are mainly distributed in the Junggar Basin. This aligns with the conclusion of Xin et al.³⁹ that altitude is the main factor influencing the distribution of high temperature, followed by latitude.

The timing of heatwaves is another important feature. Besides the HWF, HWD, and HWS, we also examined the HWFT and HWLT in Xinjiang from 1961 to 2020. Early heatwaves may have had a greater negative impact on human health than later heatwaves. This may be due to the fact that human have little opportunity to acclimatize to them⁴⁰. It is revealed that the HWFT in Xinjiang occurs mostly from early June to early July. Compared with other regions in China, the heatwave occurrence dates in Xinjiang are the same as those in North China, later than those in Southwestern China, and earlier than those in South China⁴¹. Generally, although the start of HWFT and the end of HWLT vary in different areas of Xinjiang, the HWLT ends later in those areas where the HWFT appears earlier. With the advanced HWFT and delayed HWLT, the impacts of heatwaves on human health are exacerbated and economic losses will increase⁴². For example, Mao et al.⁸ found that high temperatures caused ice melt flooding in the Tarim River Basin in 2015, and resulted in various degrees of damage to rail and road traffic, as well as water facilities.

Heatwaves are graded according to the magnitude of the HI, and it is revealed that the number of heatwave days increases from 1961 to 2020, regardless of the heatwave grade. In terms of the number of days and affected areas, the LHW is the most, followed by MHW, and SHW is the least. However, the number of SHW days in 2015 is not only the most for the period of 1961–2020, but also more than the number of MHW days in that year. This impacts the yields and quality of growing crops such as corn, cotton, and grapes⁴³. Also, the number of patients with airway diseases and cerebrovascular diseases due to heatwaves increased significantly. According to the study of Liu et al.²¹, with the intensification of global warming, heatwave affected areas will expand, and more severe heatwaves are likely to occur in the future. LHW may occur in regions that have not previously experienced heatwaves, whereas the original LHW may be transformed to MHW or even SHW. An increase in the different grades of heatwaves in the future may have serious deleterious impacts on agricultural livelihoods and human health in Xinjiang.

Heatwaves have been responsible for more annual deaths than other natural disasters in many areas of the world⁴⁴, and the PEH in Xinjiang shows an increasing trend. Influenced by the geographic pattern of 'mountain-oasis-desert', the PEH is not distributed in the desert areas where heatwaves are frequent but concentrated in the oasis regions⁴⁵. Areas with high PEH (10^5 person-days or more) are primarily located in the Kashgar, Aksu, and Hotan, mainly because these areas are predominantly agricultural and have a dense population distribution³¹. Factors influencing changes in the PEH vary with regions⁴⁶. In Europe, where population changes are relatively small or are even decreasing, the climate effect is the predominant driver for the increases in exposure. Whereas in many parts of Oceania and North Asia, changes in the PEH are mostly the result of population effects⁴⁷. Our study shows that the PEH changes in Xinjiang are mostly dominated by the climate effect, followed by the population effect. This is consistent with the finding that the highest PEH is not in 2020 with the highest population, but in 2015 with the longest HWD.

Methods

Study area. The Xinjiang Uygur Autonomous Region (34° N–50° N, 73° E–96° E) is situated in Northwestern China (Fig. 12) with an area of approximately 1.6 million km², which is the largest province in China. 'Three Mountains and Two Basins' is the major geographic feature of Xinjiang, with the Altai Mountains on the northern boundary and Kunlun Mountains on the southern boundary. The Tianshan Mountains between them is the natural geographical dividing line between the Junggar and Tarim Basins. It is customary to refer to the north of the Tianshan Mountains as Northern Xinjiang, the south as Southern Xinjiang, and Turpan and Hami as Eastern Xinjiang. Since Xinjiang is deep inland and far from the sea, it is highly sensitive to climate change⁴⁸. The region has the typical arid and semi-arid continental climate, with scarce water resources, strong solar radiation, intense evaporation, and a fragile ecological environment⁴⁹. It is extremely hot in the summer, with the highest temperature recorded as 50.5 °C in 2017.

Population growth is essential for economic and social development. The population of Xinjiang has grown steadily in recent years. According to national censuses data, the population of Xinjiang was 18.46 million in 2000 and 25.85 million in 2020, which is an increase of 7.39 million⁵⁰. The distribution of the population in Xinjiang is influenced by the natural geographical pattern of 'mountain-oasis-desert', which is mainly concentrated in the oasis region⁵¹. Furthermore, due to the more developed economy and habitable climate in Northern Xinjiang, its population density is significantly higher than that of Southern Xinjiang and Eastern Xinjiang, where Urumqi, Turpan, Karamay, and Kashgar are densely populated.

Data. The daily maximum temperature (Tmax) and relative humidity (RH) data from 1961 to 2020 are obtained from the China Meteorological Data Service Center (<http://data.cma.cn>). This dataset has a high spatial resolution of 0.25° × 0.25° and its quality control is strictly regulated by Wu et al.⁵². It is based on interpolations

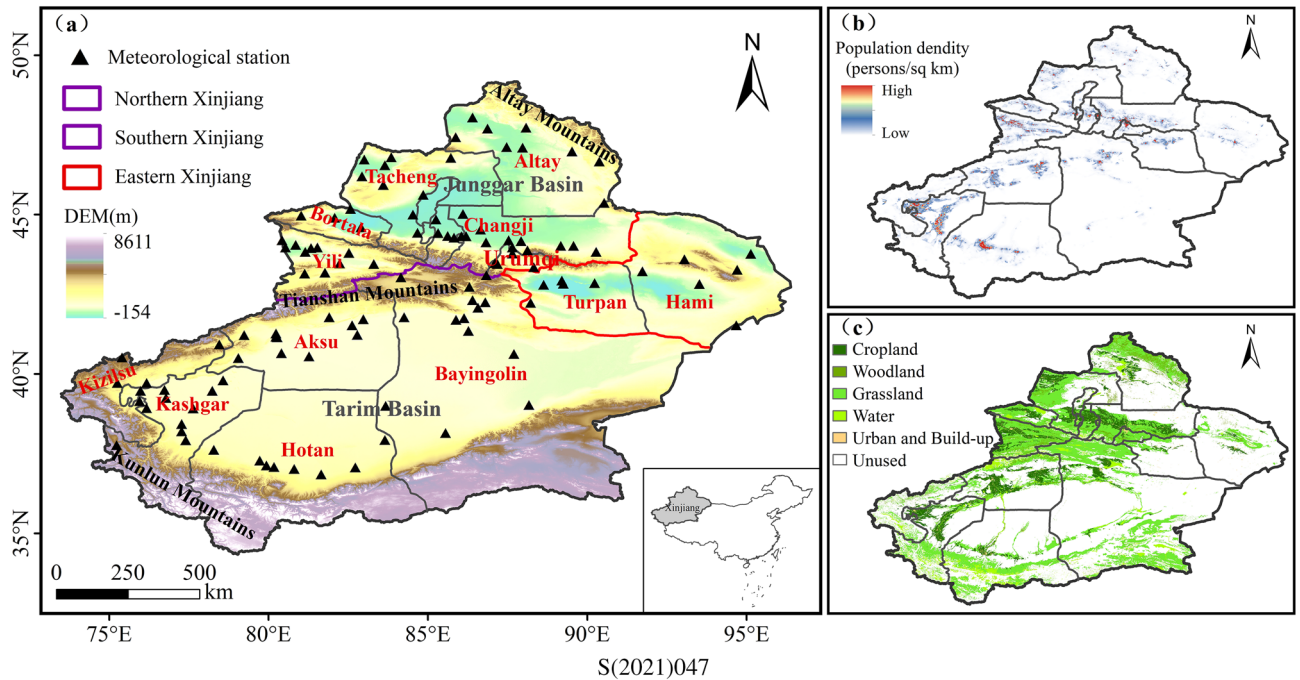


Figure 12. Maps of the study region. (a) Topographic features of Xinjiang and subregional divisions: Northern Xinjiang, Southern Xinjiang, and Eastern Xinjiang. (b) Population density. (c) Vegetation types.

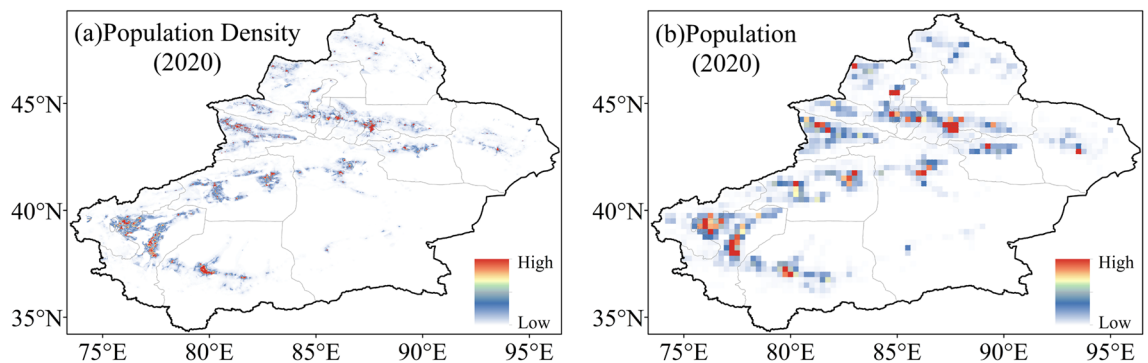


Figure 13. (a) Spatial patterns of population density in 2020. (b) Spatial patterns of population in 2020.

from over 2400 meteorological stations in China, where the climatology is initially interpolated by thin plate smoothing splines, after which a gridded daily anomaly is derive via the angular distance weighting (ADW) method and add to the climatology to obtain the final dataset. The standard map services are provided by the National Platform for Common Geospatial Information Services stand (<https://www.tianditu.gov.cn>).

High-resolution gridded population dataset for 2001 to 2020 are obtained from the WorldPop (<https://www.worldpop.org>). The dataset translates official census data and a spatial auxiliary to a grid through a random forest model. The spatial auxiliary dataset includes settlement locations and ranges, satellite nighttime lighting data, land cover data, as well as road and building maps⁵³. Many organizations and institutions employ the dataset for study since it is the most reliable long-term data series available^{54,55}. Due to computational restraints, the Worldpop data are calculated as population in the 0.25° × 0.25° grid (Fig. 13).

Methods. There is no established uniform definition of a heatwave due to the variable acclimatization and adaptability of certain population in different regions^{47,56}. For this study, in consideration of the ‘warming-wetting’ climate trend in Xinjiang⁵⁷, the heatwave index (HI) proposed by Huang et al.⁵⁸ is used to identify heatwaves. The index is calculated by Eq. (1).

$$HI = 1.2 \times (TI - TI') + 0.35 \sum_{i=1}^{N-1} 1/nd_i(TI_i - TI') + 0.15 \sum_{i=1}^{N-1} 1/nd_i + 1 \quad (1)$$

where TI is the torridity index of the current day, TI' is the critical value of TI , TI_i is the TI of the next i day before the current day, nd_i is the number of days before the current day, and N is the number of continuous hot weather days.

The torridity index for the RH ($\leq 60\%$) is obtained using the following formula:

$$TI = 1.8 \times T_{\max} - 0.55 \times (1.8 \times T_{\max} - 26) \times (1 - 0.6) + 32 \quad (2)$$

For conditions where the RH is $> 60\%$, the following formula is used:

$$TI = 1.8 \times T_{\max} - 0.55 \times (1.8 \times T_{\max} - 26) \times (1 - RH) + 32 \quad (3)$$

where T_{\max} is the daily maximum temperature ($^{\circ}\text{C}$), RH is the relative humidity (%).

The TI' is used to judge whether it is high temperature or hot weather. When TI is greater than TI' , it means that the given day reaches the high temperature state and is considered as hot weather. The quantile method is used to calculate TI' , the following formulas are used:

$$\hat{Q}_i(p) = (1 - \gamma)X_{(j)} + \gamma X_{(j+1)} \quad (4)$$

$$j = \text{int} \left[p \times n + \frac{1+p}{3} \right] \quad (5)$$

$$\gamma = p \times n + \frac{1+p}{3} - j \quad (6)$$

where $\hat{Q}_i(p)$ is the i th quantile, X denotes the sample sequence of the TI in ascending order, p is the 50% quantile, n is the length of TI series, j is the j th TI , γ is the weight of the $(j + 1)$ th number.

To measure the effects of various meteorological conditions on the socioeconomic status and human health, heatwaves are classified by three grades according to the magnitude of the HI, as listed in Table 2.

Heatwave metrics. To gain a more holistic perspective of the changes in heatwaves according to previous studies^{59,60}, we select five metrics for their quantification (Table 3).

Population exposure to heatwaves (PEH). PEH is defined as the exposure of population in heatwave-prone areas. That is, PEH can be computed by multiplying the heatwave days and the population for each grid⁶¹, where the units of exposure are person-days. The spatial resolution of PEH was set at $0.25^{\circ} \times 0.25^{\circ}$.

Changes in the PEH are determined not only by the magnitude and spatial distribution of population but also by climate change⁶². We adopt the method from Jones et al.¹⁹ to measure the impacts of climate and population on the PEH. The effects of changes in the PEH are divided into three parts.

- (1) The climate effect, which allows heatwave days to change over time but leaving the population fixed at the base period level.
- (2) The population effect, which allows the population to change but leaving heatwave days fixed at the base period level.
- (3) The interactive effect, which is defined as the total exposure change minus the summation of the changes in climate and population.

Grade	Heatwave index	Description
Light heatwave	$2.8 \leq HI < 6.5$	A certain impact on public health and social-economic activities
Moderate heatwave	$6.5 \leq HI < 10.5$	A relatively serious impact on public health and social-economic activities
Strong heatwave	$HI \geq 10.5$	A serious and harmful impact on public health and social-economic activities

Table 2. Classification standard of heatwaves.

Metric shorthand	Metric name	Metric definition
HWF	Heatwave frequency	Total number of the heatwaves in a season
HWD	Heatwave duration	Total number of contiguous days from start to end of the heatwave
HWS	Heatwave season length	Number of days from the first to the last heatwave in any given year
HWFT	First heatwave timing	Timing of the first heatwave day in a season
HWLT	Last heatwave timing	Timing of the last heatwave day in a season

Table 3. Heatwave metrics.

To facilitate comparison, we select the interval from 2001 to 2005 as the base period (T0). The comparison periods are 2006–2010 (T1), 2011–2015 (T2), and 2016–2020 (T3), respectively.

The decomposition for PEH changes is calculated according to Eq. (7)

$$\Delta E_{pop} = P_j \times C_j - P_i \times C_i = P_i \times \Delta C + C_i \times \Delta P + \Delta P \times \Delta C \quad (7)$$

where ΔE_{pop} represents the total change in PEH. P_i and C_i represent the population and the number of heatwave days in period i , respectively. P_j and C_j represent the population and the number of heatwave days in period j , respectively. ΔP and ΔC represent the changes in population and the number of heatwave days from period i to period j , respectively. $P_i \times \Delta C$ represents the climate effect, $C_i \times \Delta P$ represents the population effect, and $\Delta P \times \Delta C$ represents the interactive effect (Supplementary information).

Therefore, the contribution rate of each factor is calculated according to:

$$CR_{cli} = \frac{|P_i \times \Delta C|}{|P_i \times \Delta C| + |C_i \times \Delta P| + |\Delta P \times \Delta C|} \times 100\% \quad (8)$$

$$CR_{pop} = \frac{|C_i \times \Delta P|}{|P_i \times \Delta C| + |C_i \times \Delta P| + |\Delta P \times \Delta C|} \times 100\% \quad (9)$$

$$CR_{cli+pop} = \frac{|\Delta P \times \Delta C|}{|P_i \times \Delta C| + |C_i \times \Delta P| + |\Delta P \times \Delta C|} \times 100\% \quad (10)$$

where CR_{cli} refers to the contribution rate of the climate effect, CR_{pop} represents the contribution rate of the population effect, and $CR_{cli+pop}$ is the contribution rate of the interactive effect.

Data availability

The data that support the findings of this study are available from the corresponding author upon reasonable request.

Received: 6 December 2022; Accepted: 25 April 2023

Published online: 06 May 2023

References

- Perkins, S. E. A review on the scientific understanding of heatwaves—Their measurement, driving mechanisms, and changes at the global scale. *Atmos. Res.* **164**, 242–267. <https://doi.org/10.1016/j.atmosres.2015.05.014> (2015).
- Wang, J. *et al.* Mapping the exposure and sensitivity to heat wave events in China's megacities. *Sci. Total Environ.* <https://doi.org/10.1016/j.scitotenv.2020.142734> (2021).
- Yang, Q., Zheng, J. & Zhu, H. Influence of spatiotemporal change of temperature and rainfall on major grain yields in southern Jiangsu Province, China. *Glob. Ecol. Conserv.* <https://doi.org/10.1016/j.gecco.2019.e00818> (2020).
- Robine, J.-M. *et al.* Death toll exceeded 70,000 in Europe during the summer of 2003. *C.R. Biol.* **331**, 171–U175. <https://doi.org/10.1016/j.crvi.2007.12.001> (2008).
- McEvoy, D., Ahmed, I. & Mullett, J. The impact of the 2009 heat wave on Melbourne's critical infrastructure. *Local Environ.* **17**, 783–796. <https://doi.org/10.1080/13549839.2012.678320> (2012).
- Barriopedro, D., Fischer, E. M., Luterbacher, J., Trigo, R. & Garcia-Herrera, R. The hot summer of 2010: Redrawing the temperature record map of Europe. *Science* **332**, 220–224. <https://doi.org/10.1126/science.1201224> (2011).
- Johnson, H. *et al.* The impact of the 2003 heat wave on mortality and hospital admissions in England. *Health Stat. Quart.* **2005**, 6–11 (2005).
- Mao, W., Chen, P. & Shen, Y. Characteristics and effects of the extreme maximum air temperature in the summer of 2015 in Xinjiang under global warming. *J. Glaciol. Geocryol.* **38**, 291–304 (2016).
- Cai, W. *et al.* The 2020 China report of the Lancet Countdown on health and climate change. *Lancet Public Health* **6**, E64–E81. [https://doi.org/10.1016/s2468-2667\(20\)30256-5](https://doi.org/10.1016/s2468-2667(20)30256-5) (2021).
- Baldwin, J. W., Dessy, J. B., Vecchi, G. A. & Oppenheimer, M. Temporally compound heat wave events and global warming: An emerging hazard. *Earths Future* **7**, 411–427. <https://doi.org/10.1029/2018ef000989> (2019).
- Masson-Delmotte, V., Zhai, P., Pirani, A., Connors, S.L., Péan, C., Berger, S., Caud, N., Chen, Y., Goldfarb, L., Gomis, M.I., *et al.* IPCC. Summary for Policymakers. In *Climate Change 2021: The Physical Science Basis*; Contribution of Working Group I to the Sixth Assessment Report of the Intergovernmental Panel on Climate Change. (2021).
- Dong, Z. *et al.* Heatwaves in Southeast Asia and their changes in a warmer world. *Earths Future.* <https://doi.org/10.1029/2021ef001992> (2021).
- Meehl, G. A. & Tebaldi, C. More intense, more frequent, and longer lasting heat waves in the 21st century. *Science* **305**, 994–997. <https://doi.org/10.1126/science.1098704> (2004).
- Gao, Y., Su, P., Zhang, A., Wang, R. & Wang, J. A. Dynamic assessment of global maize exposure to extremely high temperatures. *Int. J. Disaster Risk Sci.* **12**, 713–730. <https://doi.org/10.1007/s13753-021-00360-8> (2021).
- Poumadere, M., Mays, C., Le Mer, S. & Blong, R. The 2003 heat wave in France: Dangerous climate change here and now. *Risk Anal.* **25**, 1483–1494. <https://doi.org/10.1111/j.1539-6924.2005.00694.x> (2005).
- Anderson, B. G. & Bell, M. L. Weather-related mortality: How heat, cold, and heat waves affect mortality in the United States. *Epidemiology* **20**, 205–213. <https://doi.org/10.1097/EDE.0b013e318190ee08> (2009).
- Anderson, G. B., Oleson, K. W., Jones, B. & Peng, R. D. Projected trends in high-mortality heatwaves under different scenarios of climate, population, and adaptation in 82 US communities. *Clim. Change* **146**, 455–470. <https://doi.org/10.1007/s10584-016-1779-x> (2018).
- Hajat, S., Kovats, R. S., Atkinson, R. W. & Haines, A. Impact of hot temperature on death in London: A time series approach. *J. Epidemiol. Community Health* **56**, 367–372. <https://doi.org/10.1136/jech.56.5.367> (2002).
- Jones, B. *et al.* Future population exposure to US heat extremes. *Nat. Clim. Chang.* **5**, 652–655. <https://doi.org/10.1038/nclimate2631> (2015).
- Tatem, A. J. WorldPop, open data for spatial demography. *Sci. Data* **4**, 170004–170004. <https://doi.org/10.1038/sdata.2017.4> (2017).

21. Liu, J., Ren, Y., Tao, H. & Shalamzari, M. J. Spatial and temporal variation characteristics of heatwaves in recent decades over China. *Remote Sensing*. <https://doi.org/10.3390/rs13193824> (2021).
22. Ding, T., Qian, W. & Yan, Z. Changes in hot days and heat waves in China during 1961–2007. *Int. J. Climatol.* **30**, 1452–1462. <https://doi.org/10.1002/joc.1989> (2010).
23. Jiang, Q., Yue, Y. & Gao, L. The spatial-temporal patterns of heatwave hazard impacts on wheat in northern China under extreme climate scenarios. *Geomat. Nat. Haz. Risk* **10**, 2346–2367. <https://doi.org/10.1080/19475705.2019.1693435> (2019).
24. Sherwood, S. C. How important is humidity in heat stress? *J. Geophys. Res. Atmos.* **123**, 11808–11810. <https://doi.org/10.1029/2018jd028969> (2018).
25. de Freitas, C. R. & Grigorieva, E. A. A comprehensive catalogue and classification of human thermal climate indices. *Int. J. Biometeorol.* **59**, 109–120. <https://doi.org/10.1007/s00484-014-0819-3> (2015).
26. Mora, C. *et al.* Global risk of deadly heat. *Nat. Clim. Change*. **7**, 501–506. <https://doi.org/10.1038/nclimate3322> (2017).
27. Barnett, A. G., Tong, S. & Clements, A. C. A. What measure of temperature is the best predictor of mortality?. *Environ. Res.* **110**, 604–611. <https://doi.org/10.1016/j.envres.2010.05.006> (2010).
28. Wang, Q., Zhai, P.-M. & Qin, D.-H. New perspectives on ‘warming–wetting’ trend in Xinjiang, China. *Adv. Clim. Change Res.* **11**, 252–260. <https://doi.org/10.1016/j.accre.2020.09.004> (2020).
29. Zhang, Q. *et al.* New characteristics about the climate humidification trend in Northwest China. *Chin. Sci. Bull.-Chin.* **66**, 3757–3771. <https://doi.org/10.1360/tb-2020-1396> (2021).
30. Li, L. & Zha, Y. Population exposure to extreme heat in China: Frequency, intensity, duration and temporal trends. *Sustain. Cities Society*. <https://doi.org/10.1016/j.scs.2020.102282> (2020).
31. Yang, Z., Lei, J., Duan, Z., Dong, J. & Su, C. Spatial distribution of population in Xinjiang. *Geogr. Res.* **35**, 2333–2346. <https://doi.org/10.11821/dlyj201612012> (2016).
32. Zhang, L., Huang, D. & Yang, B. Future population exposure to high temperature in China under RCP4.5 scenario. *Geograph. Res.* **35**, 2238–2248. <https://doi.org/10.11821/dlyj201612004> (2016).
33. Tao, H. *et al.* Observed changes in maximum and minimum temperatures in Xinjiang autonomous region, China. *Int. J. Climatol.* **37**, 5120–5128. <https://doi.org/10.1002/joc.5149> (2017).
34. Chen, Y., Shao, W., Cao, M. & Lyu, X. Variation of summer high temperature days and its affecting factors in Xinjiang. *Arid Zone Res.* **37**, 58–66. <https://doi.org/10.13866/j.azr.2020.01.07> (2020).
35. Zhao, G.N., Li, B.Z., Kong, P., Xia, L.J., Zhan, M.J. Population exposure to large-scale heatwaves in China for 1961–2015. in *The 5th International Conference on Water Resource and Environment (WRE 2019)* **2019**, 344. <https://doi.org/10.1088/1755-1315/344/1/012073>.
36. Luo, M. *et al.* Observed heatwave changes in arid northwest China: Physical mechanism and long-term trend. *Atmos. Res.* <https://doi.org/10.1016/j.atmosres.2020.105009> (2020).
37. Zhou, W. & Cao, F. Effects of changing spatial extent on the relationship between urban forest patterns and land surface temperature. *Ecol. Indicators*. <https://doi.org/10.1016/j.ecolind.2019.105778> (2020).
38. Shen, W. *et al.* Local land surface temperature change induced by afforestation based on satellite observations in Guangdong plantation forests in China. *Agric. Forest Meteorol.* <https://doi.org/10.1016/j.agrformet.2019.107641> (2019).
39. Xin, Y. *et al.* Analysis on the spatiotemporal change and multi scale abrupt change of high temperature days in North Xinjiang. *Arid Zone Res.* **25**, 438–446. <https://doi.org/10.13866/j.azr.2008.03.009> (2008).
40. Campbell, S., Remenyi, T. A., White, C. J. & Johnston, F. H. Heatwave and health impact research: A global review. *Health Place* **53**, 210–218. <https://doi.org/10.1016/j.healthplace.2018.08.017> (2018).
41. Jia, J. & Hu, Z. Spatial and temporal features and trend of different level heat waves over China. *Adv. Earth Sci.* **32**, 546–559. <https://doi.org/10.11867/j.issn.1001-8166.2017.05.0546> (2017).
42. Fan, J., Min, J., Yang, Q., Na, J. & Wang, X. Spatial-temporal relationship analysis of vegetation phenology and meteorological parameters in an agro-pasture ecotone in China. *Remote Sensing*. <https://doi.org/10.3390/rs14215417> (2022).
43. Shang, L., Huang, Y. & Mao W. Features of the snow and ice meltwater flood caused by high temperature in the Southern Xinjiang Region during the summer of 2015. *J. Glaciol. Geocryol.* **38**, 480–487. <https://doi.org/10.7522/j.issn.1000-0240.2016.0054> (2016).
44. Basu, R. & Samet, J. M. Relation between elevated ambient temperature and mortality: A review of the epidemiologic evidence. *Epidemiol. Rev.* **24**, 190–202. <https://doi.org/10.1093/epirev/mxf007> (2002).
45. Lu, D. *et al.* Academic debates on Hu Huanyong population line. *Geogr. Res.* **35**, 805–824. <https://doi.org/10.11821/dlyj201605001> (2016).
46. Park, C. E. & Jeong, S. Population exposure projections to intensified summer heat. *Earth's Future*. <https://doi.org/10.1029/2021ef002602> (2022).
47. Ma, F. & Yuan, X. Impact of climate and population changes on the increasing exposure to summertime compound hot extremes. *Sci. Total Environ.* **772**, 145004. <https://doi.org/10.1016/j.scitotenv.2021.145004> (2021).
48. Shen, Y.-J. *et al.* Review of historical and projected future climatic and hydrological changes in mountainous semiarid Xinjiang (northwestern China), central Asia. *CATENA* <https://doi.org/10.1016/j.catena.2019.104343> (2020).
49. Chen, D. & Dai, Y. Characteristics of Northwest China rainfall intensity in recent 50 years. *Chin. J. Atmos. Sci.* **33**, 923–935. <https://doi.org/10.3878/j.issn.1006-9895.2009.05.04> (2009).
50. Statistics Bureau of Xinjiang Uygur Autonomous Region, Xinjiang Statistical Yearbook 2021. (2022-7-1). <http://tj.xinjiang.gov.cn/tj/rkxyug/202203/a78c402be9d44ca58ff431751698d3ca.shtml>.
51. Wei, H. *et al.* Linking ecosystem services supply, social demand and human well-being in a typical mountain-oasis-desert area, Xinjiang, China. *Ecosyst. Services* **31**, 44–57. <https://doi.org/10.1016/j.ecoser.2018.03.012> (2018).
52. Wu, J. & Gao, X.-J. A gridded daily observation dataset over China region and comparison with the other datasets. *Chin. J. Geophys.-Chin. Edition* **56**, 1102–1111. <https://doi.org/10.6038/cjg20130406> (2013).
53. Gaughan, A. E. *et al.* Spatiotemporal patterns of population in mainland China, 1990 to 2010. *Sci. Data*. <https://doi.org/10.1038/sdata.2016.5> (2016).
54. Chen, B. *et al.* Contrasting inequality in human exposure to greenspace between cities of Global North and Global South. *Nat. Commun.* **13**, 4636. <https://doi.org/10.1038/s41467-022-32258-4> (2022).
55. Rentschler, J., Salhab, M. & Jafino, B. A. Flood exposure and poverty in 188 countries. *Nat. Commun.* **13**, 3527. <https://doi.org/10.1038/s41467-022-30727-4> (2022).
56. Tong, S., Wang, X. Y. & Barnett, A. G. Assessment of heat-related health impacts in Brisbane, Australia: Comparison of different heatwave definitions. *PLoS ONE* <https://doi.org/10.1371/journal.pone.0012155> (2010).
57. Shi, Y., Shen, Y. & Hu, R. Preliminary study on signal, impact and foreground of climatic shift from warm-dry to warm-humid in Northwest China. *J. Glaciol. Geocryol.* **24**, 219–226. <https://doi.org/10.7522/j.issn.1000-0240.2002.0044> (2002).
58. Huang, Z., Chen, H., Tian, H. Research on the heat wave index. *Meteorol. Mon.* **37**, 345–351 (2011).
59. Shafei Shiva, J., Chandler, D. G. & Kunkel, K. E. Localized changes in heat wave properties across the United States. *Earth's Future* **7**, 300–319. <https://doi.org/10.1029/2018ef001085> (2019).
60. Reddy, P. J., Perkins-Kirkpatrick, S. E. & Sharples, J. J. Intensifying Australian heatwave trends and their sensitivity to observational data. *Earth's Future*. <https://doi.org/10.1029/2020ef001924> (2021).
61. Weber, T. *et al.* Analysis of compound climate extremes and exposed population in Africa under two different emission scenarios. *Earth's Future*. <https://doi.org/10.1029/2019ef001473> (2020).

62. Liu, Z. *et al.* Global and regional changes in exposure to extreme heat and the relative contributions of climate and population change. *Sci. Rep.* 7, 43909. <https://doi.org/10.1038/srep43909> (2017).

Acknowledgements

This work was supported by the Key Research and Development Program of Xinjiang Uygur Autonomous Region, China (2022B03030) and the West Light Foundation of the Chinese Academy of Sciences (Grant numbers 2019-XBYJRC-001, 2019-XBQNXZ-B-0004).

Author contributions

D.D., H.T. and Z.Z. conceived the study. D.D. and H.T. prepared the database. D.D. created the figures and analyzed the results. Z.Z. improved the structure of the paper. All authors have read and agreed to the published vision of the manuscript.

Competing interests

The authors declare no competing interests.

Additional information

Supplementary Information The online version contains supplementary material available at <https://doi.org/10.1038/s41598-023-34123-w>.

Correspondence and requests for materials should be addressed to Z.Z.

Reprints and permissions information is available at www.nature.com/reprints.

Publisher's note Springer Nature remains neutral with regard to jurisdictional claims in published maps and institutional affiliations.



Open Access This article is licensed under a Creative Commons Attribution 4.0 International License, which permits use, sharing, adaptation, distribution and reproduction in any medium or format, as long as you give appropriate credit to the original author(s) and the source, provide a link to the Creative Commons licence, and indicate if changes were made. The images or other third party material in this article are included in the article's Creative Commons licence, unless indicated otherwise in a credit line to the material. If material is not included in the article's Creative Commons licence and your intended use is not permitted by statutory regulation or exceeds the permitted use, you will need to obtain permission directly from the copyright holder. To view a copy of this licence, visit <http://creativecommons.org/licenses/by/4.0/>.

© The Author(s) 2023